3
Vibrations in sp^2 Nanocarbons

Although the inelastic process of Raman scattering of light can originate from the creation or annihilation of polaritons, plasmons, magnons or any elementary excitations in molecules and solids, it is the phonons, which are the quanta of atomic vibration that are the main source of Raman spectra in the literature, and are the focus of this chapter. In sp^2 nanocarbons, the phonons, like the electrons, depend on the atomic structure and the Raman phonon spectra can be used to study the similarities and differences between the various materials within the sp^2 nanocarbon family, thereby providing a sensitive tool to distinguish one member of the sp^2 nanocarbon family from another.

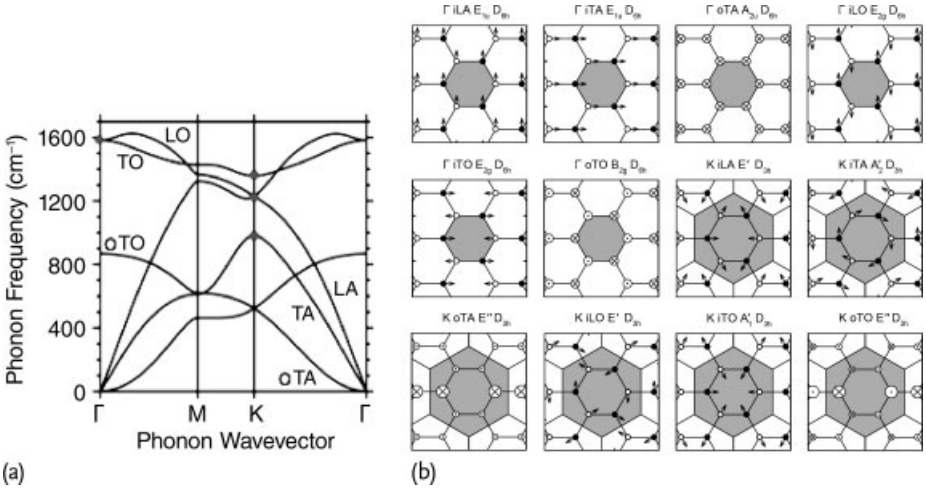

Figure 3.1 (a) Phonon dispersion relations for graphene and (b) the eigenvectors for the in-plane phonons relevant to the high symmetry Γ point and K (K') points of the Brillouin zone. Each of these twelve modes is labeled and their atom displacements are indicated [117]. i/o stands for in-plane/out-of-plane; T/L stands for transversal/longitudinal; A/O stands for acoustic/optical. The other symbols are symmetry assignments according to group theory, as discussed in Chapter 6.

Raman Spectroscopy in Graphene Related Systems. Ado Jorio, Riichiro Saito, Gene Dresselhaus, and Mildred S. Dresselhaus

ISBN: 978-3-527-40811-5

Figure 3.1a shows the phonon dispersion relations $\omega(q)$ of monolayer graphene, the building block of many of the other carbon sp^2 nanostructures, calculated within the so-called *force constant model* [31, 116].

There are six branches in these phonon dispersion relations because the crystal has a unit cell with two distinct atom sites (A and B). The six eigenvectors *at* the Γ point ($q = 0$, that is the wavelength, $\lambda \to \infty$) consist of three translations of the crystal along x, y, z, which have no restoring force and, consequently, zero frequency, plus three vibrational modes, two of which are degenerate. The Γ point phonons shown in Figure 3.1 include the stretching of the C–C bond in the graphene unit cell, and the phonons are denoted by LO or TO according to whether the atomic vibrations are along or perpendicular to the direction of the wave vector $\boldsymbol{q}$ (not shown). Graphene is a nonionic crystal, since the unit cell is formed by two atoms of the same type, and because of the nonionic behavior of the graphene crystal, the LO and TO phonon modes are degenerate at the Γ point.[1)] For the K point phonons, $q \neq 0$ and there is a phase factor in the phonon eigenfunctions from one unit cell relative to the neighboring unit cell.

The brief description above introduces the picture of how to treat phonons in a crystal, and the goal of this chapter is to describe the vibrational structure of sp^2 carbons. Similar to what was covered in Chapter 2, we aim in this chapter to capture the fundamental concepts for the phonon dispersion from the energy levels for a very simple molecule and then to build the phonon dispersion structure of a crystal, as presented in Figure 3.1. Therefore, we begin in Section 3.1 by briefly reviewing some basic concepts: the harmonic oscillator, which describes the fundamental physics of molecular vibrations (Section 3.1.1); the concept of normal modes from molecules to crystals (Section 3.1.2); the force constant model (Section 3.1.3), in which interatomic forces are represented by spring constants to calculate the phonon dispersion relations in crystals. With these basic concepts in place, we develop the force constant model for graphene (Section 3.2). Like the tight-binding approximation for the electronic structure (Chapter 2), the force constant model is simple enough to be solved analytically, thus giving an understanding about how to build the phonon structure of graphene. Again similar to electrons, phonon confinement takes place in carbon nanotubes and can be described, as a first approximation, by the zone-folding procedure, which is developed in Section 3.4. Finally, both the zone-folding and the force constant model have their limitations which are discussed in Sections 3.4.2 and 3.5. The force constant model, with connections also made to 3D graphite, can be expressed quite accurately by increasing the number of neighbors and the number of force constants, but it fails when effects like the electron–phonon coupling are important. Such a failure is actually very important for interpreting the Raman spectroscopy of sp^2 carbon nanotubes, and is briefly discussed in this chapter. Further discussion is given in more detail throughout the book whenever new aspects of the electron–phonon interaction are needed to explain specific phenomena associated with the Raman spectra of sp^2

1) In the case of an ionic crystal, like NaCl, the LO mode has a higher frequency than the TO mode because of the Coulomb interaction between the ions. The LO-TO splitting is then related to the dielectric constant through the Lydane–Sacks–Teller (LST) theory [118].

carbons. Many basic textbooks on Raman spectroscopy are available to supplement the presentation provided in this book which is focused on sp^2 carbons [119–122].

3.1
Basic Concepts: from the Vibrational Levels in Molecules to Solids

To provide an overview of the basics, we first review the use of a harmonic oscillator (Section 3.1.1), which is important for defining phonons and describing phonon amplitudes and displacements that are needed for Raman intensity calculations. Then we discuss the normal vibrational modes in molecules and how the number of normal modes evolves from small molecules to a crystal with an "infinite" number of atoms, thereby building the phonon dispersion relations in crystals (Section 3.1.2). Finally we describe the force constant model for vibrations in general terms (Section 3.1.3).

3.1.1
The Harmonic Oscillator

The atomic motion in molecules and solids is described in terms of the normal modes of vibration, which are represented by an orthogonal set of harmonic oscillators. Classically, a harmonic oscillator can be described by

$$m\frac{d^2(x - x_{\mathrm{eq}})}{dt^2} = -K(x - x_{\mathrm{eq}}) \,, \tag{3.1}$$

where m, x_{eq} and K are, respectively, the mass, the equilibrium position (see Figure 3.2) and the force constant for the harmonic oscillator. A solution of Eq. (3.1) is given by

$$x(t) = x_{\mathrm{eq}} + A\cos(\omega t + \phi), \quad \text{and} \quad \omega \equiv \sqrt{\frac{K}{m}} \,, \tag{3.2}$$

where A, ω and ϕ are, respectively, the amplitude, the frequency and the phase of the vibration. A and ϕ are determined by the initial conditions at time $t = 0$.

However, the description above does not take into account the quantum nature of the atoms, which can be described by solving the time-dependent Schrödinger

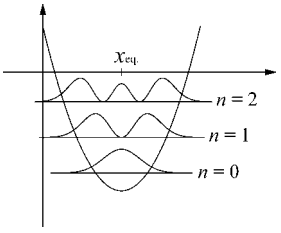

Figure 3.2 The potential energy for a harmonic oscillator showing the quantized energy levels for a molecular mode vibration. The waves associated with each energy level display the probability to find the interatomic distance at a given x value.

equation for the quantum harmonic oscillator (HO)

$$\left[-\frac{\hbar^2}{2m}\frac{\partial^2}{\partial x^2}+\frac{1}{2}Kx^2\right]\Psi_n = E_n\Psi_n, \quad (n=0,1,2,\ldots)\,, \tag{3.3}$$

in which Ψ_n is a wave function of the harmonic oscillator and n labels the quantum state of the harmonic oscillator. The vibrational amplitude for Ψ_n, which is proportional to $\sqrt{n}$, is quantized and the different vibrational levels are described by the number of vibrational quanta, called phonons, and quantified by the quantum number n (see Figure 3.2).

To account for the quantum nature of phonons and their energies, we introduce the annihilation operator a and the creation operator $a^\dagger$ which, respectively, annihilates one phonon or creates one phonon of energy $\hbar\omega$:

$$a = \frac{p - i\omega m x}{\sqrt{2\hbar\omega m}}, \quad \text{and} \quad a^\dagger = \frac{p + i\omega m x}{\sqrt{2\hbar\omega m}}\,. \tag{3.4}$$

The annihilation operator a lowers the quantum number of the state $|n\rangle \equiv \Psi_n$ to $|n-1\rangle$, while the creation operator $a^\dagger$ increases the quantum number of the state $|n\rangle$ to $|n+1\rangle$. Since the commutator $[p, x] = \hbar/i$, it follows that

$$[a, a^\dagger] = 1\,, \tag{3.5}$$

so that the Hamiltonian for the harmonic oscillator in Eq. (3.3) can be written in terms of the operators a and $a^\dagger$ as:

$$\mathcal{H} = \frac{1}{2m}\left[(p + i\omega m x)(p - i\omega m x) + m\hbar\omega\right] \tag{3.6}$$

$$= \hbar\omega[a^\dagger a + 1/2]\,. \tag{3.7}$$

Considering $N = a^\dagger a$ to be the number operator, the Hamiltonian in Eq. (3.7) can be written as

$$\mathcal{H}|n\rangle = \hbar\omega[N + 1/2]|n\rangle = \hbar\omega(n + 1/2)|n\rangle\,. \tag{3.8}$$

Thus the eigenvalues for the harmonic oscillator are written as:

$$E = \hbar\omega(n + 1/2), \qquad (n = 0, 1, 2, \ldots) \tag{3.9}$$

as shown in Figure 3.2. Here n corresponds to the number of phonons with frequency ω. The phonon amplitude will be related to the number of phonons n, which depends on the phonon energy and temperature, as given by the Bose–Einstein distribution function (see Section 4.3.2.1).

3.1.2 Normal Vibrational Modes from Molecules to a Periodic Lattice

In a molecule with N atoms, there exist $3N-6$ degrees of freedom for vibrations. Of these $3N-6$ modes, 6 correspond to the degrees of freedom for the translation and rotation of the center of mass, which either have no restoring force (zero frequency

for translations) or have very small frequencies (rotations).[2] Any atomic motion of the molecule can be expressed by a linear combination of these $3N-6$ independent, orthogonal vibrations, which we call normal modes.

As a simple example, we discuss the molecular vibrations of the NO molecule, which is an exception to the $3N-6$ rule, but has $3N-5$ normal modes. Having two atoms, the NO molecule has 6 degrees of freedom for atomic motion in three dimensions, but has only one vibrational mode. Three degrees of freedom are associated with translations of the molecule along x, y and z, and only two degrees of freedom involve molecular rotations around the x and y axes. Rotation around the z (N–O bond) axis does not represent motion for a linear molecule, which therefore has $3N-5=1$ vibrational modes. The vibrational mode is represented by the N–O bond stretching vibration, which is a breathing mode that does not alter the symmetry of the molecule but only changes the bond length (dipole moment).

Increasing the size of the molecule from two to three atoms, we now consider the CO_2 molecule, which is also a linear molecule with the carbon atom at the center and each of the oxygen atoms (along the z direction, for example) located at distances $\pm z_0$ from the carbon atom. In this case, there are 9 degrees of freedom, 4 of which are vibrational. This gives rise to a symmetric breathing mode with the C atom remaining static and the oxygen moving in $\pm z$ directions to preserve the center of mass. A second mode is the antisymmetric stretch mode with the carbon atom moving for example in the $+z$ direction when the two oxygen atoms move in the $-z$ direction to preserve the center of mass. In addition, there is a doubly degenerate bending mode where the two oxygen and the carbon atoms vibrate in the directions normal to the molecular axis (i. e., the $\pm x$ and $\pm y$) directions. In this case the bending and antisymmetric stretch modes that create a dipole moment are infrared-active and the symmetric stretching mode that transforms as a symmetric second rank tensor are Raman-active. These symmetry concepts behind Raman activity can be described by group theory and will be discussed in Chapter 6.

Finally, finding the normal modes of large and complex molecules, such as proteins, is not an easy task because of the large number of degrees of freedom. In cases like that, it is common to find the spectral features identified with the stretching and bending of local bonds (e. g., C=C, C−H, C=O, etc.) rather than the complete molecular normal modes. Crystals have a large number of atoms (ideally infinite), but periodic systems are, again, quite simple to describe in terms of molecules in real and reciprocal space, and require the use of *phonon dispersion relations*, $\omega(q)$ where q is the phonon wave vector.

The Bloch theorem developed in Section 2.1.5 for electrons can be used to describe the vibrational structure of crystalline solids. The same concepts, such as the unit cell in real and reciprocal space, the Brillouin zone, etc., are used to describe the vibrational structure, but the name *branches* is used in place of bands to designate the phonon dispersion relations. Consider N as the number of atoms in the unit cell, and $N_\Omega \sim 10^{23}$ per mole, as the number of unit cells in a mole of crystal.

2) Typical rotational energies are on the order of $\sim$ 1 meV and occur at far-infrared frequencies. The vibrational modes of molecules are observed in the mid-IR range, typically in the range 20–100 meV, and are the usual subject of study for molecular Raman spectroscopy.

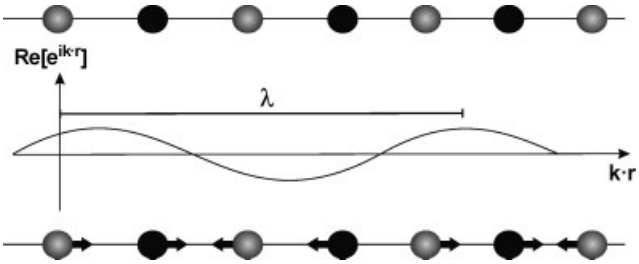

Figure 3.3 Schematic phonon eigenvector for a 1D crystal with two atoms in the unit cell. The phonon mode is the longitudinal acoustic (LA) phonon branch with $q = 8\pi/9a$ ($\lambda = 9a/4$).

There will then be $3 \times N_\Omega \times N$ vibrational modes, which is infinite for a crystal of infinite size, but the quasi-infinite number of vibrational modes are grouped into the various phonon branches. While the number of electronic bands is defined by the number of electrons in the unit cell, the number of phonon branches is defined by the number of atoms (N) in the unit cell. The difference between one phonon to another within the branch is not given by the atomic motion within the unit cell, but rather by the change in the phase of the vibration from one unit cell to the next. A schematic phonon eigenvector for a hypothetical 1D crystal with $N = 2$ is shown in Figure 3.3, which should be compared to Figure 2.5 for *s* and *p* electrons. This difference among phonons within the unit cell is described by phonon wave vectors, which are usually labeled $\boldsymbol{q}$ (where $\boldsymbol{k}$ is used for the electron wave vector), and their energies are given by $E_{\boldsymbol{q}} = \hbar\omega_{\boldsymbol{q}}$. A plot of $\omega_{\boldsymbol{q}}$ vs. $\boldsymbol{q}$, such as in Figure 3.1a, gives the phonon dispersion relations for graphene [31].

There are $3 \times N_\Omega$ modes related to the translation of N_Ω unit cells along the 3 directions of real space. However, only the translations along x, y and z with infinite wavelength λ (i. e., for the null wave vector $q = 0$ at the Γ point) represent a crystal translation (no restoring force, zero frequency). All the other $3N_\Omega - 3$ modes actually have a restoring force from the neighboring unit cells, and they are all vibrational modes grouped in three branches called *acoustic branches*, since they are related to the transport of acoustic waves at long wavelengths.[3] In general, the sound velocity for *longitudinal waves* is faster than that for *transverse waves*. In high symmetry crystals such as 2D graphene and 3D graphite we define the wave propagation direction by the wave vector $\boldsymbol{q}$, and for a given $\boldsymbol{q}$ we can define one longitudinal acoustic (LA) branch, where the vibrational amplitude is parallel to the wave propagation direction $\boldsymbol{q}$, and two transverse acoustic (TA) branches, whose amplitudes are perpendicular to $\boldsymbol{q}$ (Figure 3.4).

The rotation of a unit cell in a crystal is not allowed. All the other $3N_\Omega N - 3N_\Omega$ modes are also vibrational modes, and they group into $3N - 3$ branches named *optical branches*, making reference to the fact that they are usually studied using optics. Like for the acoustic branches, the optical branches can be classified into longitudinal and transversal modes, using the general nomenclatures LO and TO, respectively (with "O" for optical replacing "A" for acoustic).

3) A long wavelength phonon would have $\lambda > 50$ cm if the velocity of sound is 10 km/s and if the highest frequency of sound is 20 kHz.

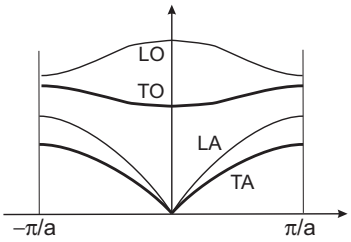

Figure 3.4 Schematic phonon dispersion relations for a hypothetical 1D crystal made by the repetition of two different atoms. The thicker lines indicate doubly degenerate branches for both the acoustic and optical branches.

As an illustration, Figure 3.4 shows the phonon dispersion relations schematically for a hypothetical 1D crystal made of two different alternating atoms (Figure 3.3). The two lower energy branches are for the acoustic phonons and two higher energy branches are for the optical phonons. Up to six branches (3 acoustic and 3 optical) are expected in 3D graphite, since we have two atoms unit cell. However, in the case of the hypothetical 1D crystal, two acoustic and two optical modes are degenerate, since atomic vibrations along x or y will have the same energies.

Another important concept is the *zone boundary of the phonon dispersion*, already discussed in Section 2.1.5, which is given in Figure 3.4 by $q = \pm\pi/a$. This boundary which we call the first Brillouin zone boundary is defined by the largest possible value for $q = 2\pi/\lambda = 2\pi/2a$. Any value larger than that can be folded back inside the $\pm\pi/a$ boundaries of the first Brillouin zone. For example, if we draw in Figure 3.3 the motion for $q = 0$ ($\lambda \to \infty$) and for $q = 2\pi/a$ ($\lambda = a$), we will see that the motion of equivalent atoms is identical.

Understanding the meaning of a phonon dispersion relation like Figures 3.1 and 3.4 is very important for Raman spectroscopy and for materials science in general, and this is the goal of Section 3.1. In the next section we introduce a model used to calculate such phonon dispersion relations for actual materials.

3.1.3
The Force Constant Model

In general, the equations of motion for the displacement of the ith atom measured from the equivalent position, $\boldsymbol{u}_i = (x_i, y_i, z_i)$ for N atoms in the unit cell is given by

$$M_i \ddot{\boldsymbol{u}}_i = \sum_j K^{(ij)}(\boldsymbol{u}_j - \boldsymbol{u}_i), \quad (i = 1, \ldots, N)\ , \tag{3.10}$$

where M_i is the mass of the ith atom and $K^{(ij)}$ represents the 3×3 force constant tensor[4] between the ith and the jth atoms. The sum over j in Eq. (3.10) is normally

4) A second rank tensor is defined by a 3×3 matrix whose elements $(K_{xx}, K_{xy}, \ldots, K_{zz})$ can be transformed as $U^{-1} K U$, where U is a unitary matrix which transforms the x, y, z coordinates into another orthogonal x', y', z' coordinate system without changing the length scale.

taken over only a few neighbor distances relative to the ith site, which for a 2D graphene sheet has been carried out up to fourth nearest neighbor interactions in [123]. In order to reproduce the experimental results, up to twentieth nearest neighbor interactions have been considered [116, 124]. In a periodic system we can perform a Fourier transform of the displacement of the ith atom with the wave number $\boldsymbol{k}'$ to obtain the normal mode displacements $\boldsymbol{u}_{\boldsymbol{k}^{(i)}}$

$$\boldsymbol{u}_i = \frac{1}{\sqrt{N_\Omega}} \sum_{\boldsymbol{q}'} e^{-i(\boldsymbol{q}'\cdot\boldsymbol{R}_i - \omega t)} \boldsymbol{u}_{\boldsymbol{q}'}^{(i)}, \qquad \text{or} \quad \boldsymbol{u}_{\boldsymbol{q}^{(i)}} = \frac{1}{\sqrt{N_\Omega}} \sum_{\boldsymbol{R}_i} e^{i(\boldsymbol{q}\cdot\boldsymbol{R}_i - \omega t)} \boldsymbol{u}_i \ , \tag{3.11}$$

in which the sum is taken over all (N_Ω) wave vectors $\boldsymbol{q}'$ in the first Brillouin zone[5] and $\boldsymbol{R}_i$ denotes the atomic position of the ith atom in the crystal. When we assume the same eigenfrequencies ω for all $\boldsymbol{u}_i$, that is $\ddot{\boldsymbol{u}}_i = -\omega^2 \boldsymbol{u}_i$, then Eq. (3.10) can be formally written by defining a $3N \times 3N$ dynamical matrix $\mathcal{D}(\boldsymbol{q})$

$$\mathcal{D}(\boldsymbol{q})\boldsymbol{u}_{\boldsymbol{q}} = 0 \ . \tag{3.12}$$

To obtain the eigenvalues $\omega^2(\boldsymbol{q})$ for $\mathcal{D}(\boldsymbol{q})$ and nontrivial eigenvectors $\boldsymbol{u}_{\boldsymbol{q}} \neq \boldsymbol{0}$, we solve the secular equation $\det\mathcal{D}(\boldsymbol{q}) = 0$ for a given $\boldsymbol{q}$ vector. It is convenient to divide the dynamical matrix $\mathcal{D}(\boldsymbol{q})$ into small 3×3 matrices $\mathcal{D}^{(ij)}(\boldsymbol{q})$, $(i, j = 1, \cdots, N)$, where we denote $\mathcal{D}(\boldsymbol{q})$ by $\{\mathcal{D}^{(ij)}(\boldsymbol{q})\}$, and from Eq. (3.12) it follows that $\mathcal{D}^{(ij)}(\boldsymbol{q})$ is expressed as:

$$\mathcal{D}^{(ij)}(\boldsymbol{q}) = \left(\sum_{j''} K^{(ij'')} - M_i \omega^2(\boldsymbol{q}) I \right) \delta_{ij} - \sum_{j'} K^{(ij')} e^{i\boldsymbol{q}\cdot\Delta\boldsymbol{R}_{ij'}} \ , \tag{3.13}$$

in which I is a 3×3 unit matrix and $\Delta\boldsymbol{R}_{ij} = \boldsymbol{R}_i - \boldsymbol{R}_j$ is the relative coordinate of the ith atom with respect to the jth atom. The vibration of the ith atom is coupled to that of the jth atom through the $K^{(ij)}$ force constant tensor. The sum over j'' is taken for all neighbor sites from the ith atom with $K^{(ij'')} \neq 0$, and the sum over j' is taken over the equivalent sites to the jth atom. The first two terms[6] of Eq. (3.13) have nonvanishing values only when $i = j$, and the last term appears only when the j'th atom is coupled to the ith atom through $K^{(ij')} \neq 0$.

In a periodic system, the dynamical matrix elements are given by the product of the force constant tensor $K^{(ij)}$ and the phase difference factor $e^{i\boldsymbol{q}\cdot\Delta\boldsymbol{R}_{ij}}$. This situation is similar to the case of the tight-binding calculation for the electronic structure where the matrix element is given by the product of the atomic matrix element and the phase difference factor (see Section 2.2.2).

5) N_Ω is the number of unit cells in the solid and thus $N_\Omega \sim 10^{23}$/mole.

6) These terms correspond to the diagonal block of the dynamical matrix. The last term in Eq. (3.13) is in the off-diagonal (ij) block of the dynamical matrix. When the ith atom has equivalent neighbor atoms in the adjacent unit cells, the last term can appear in the diagonal block of the dynamical matrix.

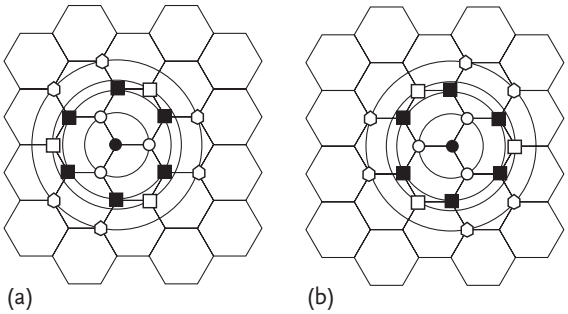

Figure 3.5 Neighbor atoms of graphene up to fourth nearest neighbors for (a) an *A* atom and (b) a *B* atom at the center denoted by solid circles. From the first to the fourth neighbor atoms, we plot 3 open circles (first neighbor), 6 solid squares (second), 3 open squares (third), and 6 open hexagons (fourth), respectively. Circles connecting the same neighbor atoms are for guides to the eye [31].

3.2 Phonons in Graphene

Now we describe the force constant model applied to graphene (two-dimensional graphite). In graphene, since there are two distinct carbon atoms, *A* and *B*, in the unit cell, we must consider six coordinates $\boldsymbol{u_k}$ (or 6 degrees of freedom) in Eq. (3.12). The secular equation to be solved is thus a 6×6 dynamical matrix $\mathcal{D}$. The dynamical matrix $\mathcal{D}$ for graphene is written in terms of the 3×3 matrices: (1) D^{AA}, (2) D^{AB}, (3) D^{BA}, and (4) D^{BB} for the coupling between (1) *A* and *A*, (2) *A* and *B*, (3) *B* and *A* and several (4) *B* and *B* atoms in the various unit cells

$$\mathcal{D} = \begin{pmatrix} D^{AA} & D^{AB} \\ D^{BA} & D^{BB} \end{pmatrix} . \tag{3.14}$$

When we consider an *A* atom, the three nearest neighbor atoms (see Figures 3.5 and 3.6) are B_1, B_2, and B_3 whose contributions to $\mathcal{D}$ are contained in D^{AB}, while the six next-nearest neighbor atoms denoted by solid squares in Figure 3.5a are all *A* atoms, with contributions to $\mathcal{D}$ that are contained in D^{AA} and so on. In Figure 3.5a, b, we show neighbor atoms up to fourth nearest neighbors for the *A* and *B* atoms, respectively. It is important to note that the *A* and *B* sites do not always appear alternately for the *n*th neighbors. In fact the third and the fourth neighbor atoms in Figure 3.5 belong to equivalent atoms.

The remaining problem is how to construct the force constant tensor $K^{(ij)}$. Here we show a simple way to obtain $K^{(ij)}$.[7] First we consider the force constant between

7) Since the determinant of the dynamical matrix is a scalar variable, the determinant should be invariant under any operation of the point group for the unit cell. Thus the proper combination of terms in the product of the force constant tensor $K^{(ij)}$ and the phase difference factor $e^{i\boldsymbol{q}\cdot\Delta\boldsymbol{R}_{ij}}$ is determined by group theory, which gives block-diagonalization in accordance with the irreducible representations of the symmetry groups of periodic structures (see Chapter 6). Further details are given in the literature for Si and Ge in [125], and for graphite in [126].

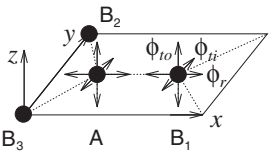

Figure 3.6 Force constants between the A and B_1 atoms on a graphene sheet. Here ϕ_r, ϕ_{ti}, and ϕ_{to} represent forces for the nearest neighbor atoms in the radial (bond-stretching), in-plane and out-of-plane tangential (bond-bending) directions, respectively. B_2 and B_3 are the nearest neighbors equivalent to B_1, whose force constant tensors are obtained by appropriately rotating the $K^{(ij)}$ tensor for A and B_1 [31].

an A atom and a nearest neighbor B_1 atom on the x axis as shown in Figure 3.6 (see also Figure 2.6a). The force constant tensor is given by

$$K^{(A,B_1)} = \begin{pmatrix} \phi_r^{(1)} & 0 & 0 \\ 0 & \phi_{ti}^{(1)} & 0 \\ 0 & 0 & \phi_{to}^{(1)} \end{pmatrix}, \tag{3.15}$$

where $\phi_r^{(n)}$, $\phi_{ti}^{(n)}$, and $\phi_{to}^{(n)}$ represent the force constant parameters in the radial (bond-stretching), in-plane and out-of-plane tangential (bond-bending) directions of the nth nearest neighbors, respectively. Here the graphene plane is the xy plane, the radial direction (x in the case of Figure 3.6) corresponds to the direction of the σ bonds (dotted lines), and the two tangential directions (y and z) are taken to be perpendicular to the radial direction. Since graphite is an anisotropic material, we introduce two parameters to describe the in-plane (y) and out-of-plane (z) tangential phonon mode, and the corresponding phase factor, $e^{i\boldsymbol{q}\cdot\Delta\boldsymbol{R}_{ij}}$, becomes $\exp(-iq_x a/\sqrt{3})$ for the B_1 atom at $(a/\sqrt{3}, 0, 0)$.

The force constant matrices for the two other nearest neighbor atoms, B_2 and B_3 are obtained by rotating the matrix in Eq. (3.15) according to the rules for a second-rank tensor

$$K^{(A,Bm)} = U_m^{-1} K^{(A,B_1)} U_m, \quad (m = 2, 3), \tag{3.16}$$

where the unitary matrix U_m is here defined by a rotation matrix around the z axis in Figure 3.6, taking the B_1 atom into the Bm atom,[8)]

$$U_m = \begin{pmatrix} \cos\theta_m & \sin\theta_m & 0 \\ -\sin\theta_m & \cos\theta_m & 0 \\ 0 & 0 & 1 \end{pmatrix}. \tag{3.17}$$

8) The formulation should be in terms of the rotation of the axes connecting an atom A to its various equivalent neighbors. However, for easy understanding, we present in Eq. (3.16) the rotation of atoms. The matrix for the rotation of the *axes* is the transpose matrix of the matrix for the rotation of *atoms*.

To make the method explicit, we show next the force constant matrix for the B_2 atom at $[-a/(2\sqrt{3}), a/2, 0]$, and U_2 is evaluated assuming $\theta_2 = 2\pi/3$,

$$K^{(A,B_2)} = \frac{1}{4}\begin{pmatrix} \phi_r^{(1)} + 3\phi_{ti}^{(1)} & \sqrt{3}(\phi_{ti}^{(1)} - \phi_r^{(1)}) & 0 \\ \sqrt{3}(\phi_{ti}^{(1)} - \phi_r^{(1)}) & 3\phi_r^{(1)} + \phi_{ti}^{(1)} & 0 \\ 0 & 0 & \phi_{to}^{(1)} \end{pmatrix}, \tag{3.18}$$

and the corresponding phase factor is given by $\exp[-iq_x a/(2\sqrt{3}) + iq_y a/2]$.

In the case of the phonon dispersion relations calculation for monolayer graphene, the interactions between two nearest-neighbor atoms are not sufficient to reproduce the experimental results, and we generally need to consider contributions from long-distance forces, such as from the nth neighbor atoms, $(n = 1, 2, 3, 4 \ldots)$.[9] To describe the twisted motion of four atoms, in which the outer two atoms vibrate around the bond of the two inner atoms as shown in Figure 3.7, contributions up to at least the fourth nearest neighbor interactions are necessary [127]. Values for the force constants [123] (see Table 3.1) are obtained by fitting the 2D phonon dispersion relations over the Brillouin zone as determined experimentally, as for example from electron energy loss spectroscopy [128], inelastic neutron scattering [123] or inelastic X-ray scattering [129, 130].

In Figure 3.8a the phonon dispersion curves for a monolayer graphene sheet, denoted by solid lines, are shown using the set of force constants in Table 3.1. In Figure 3.8b the corresponding density of phonon states is plotted per C atom per cm^{-1}, where the energy is in units of cm^{-1}. The calculated phonon disper-

Table 3.1 Force constant parameters for 2D graphene out to fourth neighbors in units of 10^4 dyn/cm [123]. Here the subscripts r, ti, and to refer to radial, transverse in-plane and transverse out-of-plane, respectively. See Figures 3.5 and 3.6.

Radial			Tangential		
$\phi_r^{(1)} =$	36.50	$\phi_{ti}^{(1)} =$	24.50	$\phi_{to}^{(1)} =$	9.82
$\phi_r^{(2)} =$	8.80	$\phi_{ti}^{(2)} =$	−3.23	$\phi_{to}^{(2)} =$	−0.40
$\phi_r^{(3)} =$	3.00	$\phi_{ti}^{(3)} =$	−5.25	$\phi_{to}^{(3)} =$	0.15
$\phi_r^{(4)} =$	−1.92	$\phi_{ti}^{(4)} =$	2.29	$\phi_{to}^{(4)} =$	−0.58

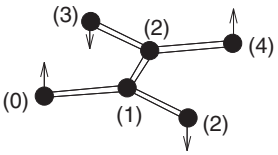

Figure 3.7 In order to describe the twisted motion of four atoms, it is necessary to consider up to at last fourth-nearest neighbor interactions. The numbers shown in the figure denote the nth nearest neighbor atoms from the leftmost zeroth atom.

9) When we consider the force constant matrix of the nth neighbor atoms, these atoms are not always located on the x (or y) axis. In that case it does not seem that we can build an initial force constant matrix as given by Eq. (3.15). This happens at the fourth neighbor atoms in graphene. However, if we consider a virtual atom on the x axis, and if we then rotate the matrix, we can get the force constant matrix without any difficulty.

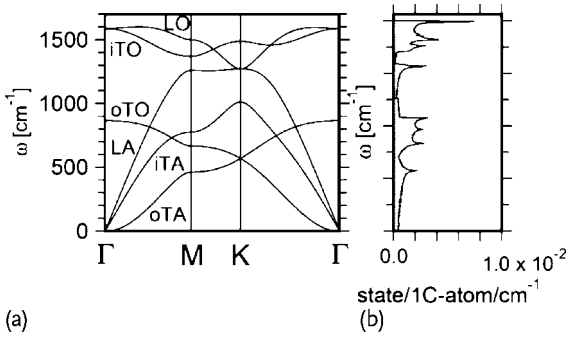

Figure 3.8 (a) The phonon dispersion curves, plotted along high symmetry directions, for a 2D monolayer graphene sheet, using the set of force constants in Table 3.1 [123]. (b) The corresponding density of states vs. phonon energy for phonon modes in units of states/1C-atom/$\text{cm}^{-1} \times 10^{-2}$ [31].

sion curves of Figure 3.8a reproduce the experimental points obtained by electron energy loss spectroscopy in general [127, 128], but are not very accurate for the optical phonons near the K point (see the difference between Figures 3.8 and 3.1 and [129]). Thus, to a first approximation the inclusion of fourth-neighbor interactions is sufficient for reproducing the phonon dispersion relations of 2D graphite, but for a very accurate description of the phonon structure near the K point, other effects have to be considered, as discussed briefly in Section 3.5.

The three phonon dispersion branches, which originate from the Γ point of the Brillouin zone (see Figure 3.8a), correspond to acoustic modes: an out-of-plane mode (oTA), an in-plane tangential (bond-bending) mode (iTA) and an in-plane longitudinal (or radial, bond-stretching) mode (iLA),[10] listed in order of increasing energy, respectively. The remaining three branches correspond to optical modes: one out-of-plane mode (oTO) and two in-plane modes (iTO and iLO).

It is noted that the oTA branch shows a q^2 energy dispersion relation around the Γ point, while the other two in-plane acoustic branches show a linear q dependence, as is normally seen for acoustic modes. One reason why we get a q^2 dependence for the out-of-plane mode is simply because this branch corresponds to a two-dimensional phonon mode and because graphite has three-fold rotational symmetry. It is clear in Eq. (3.16) that all rotations U are within the x, y plane in the case of monolayer graphene. Thus the force constant matrix can be decomposed into a 2×2 matrix of x, y components and a 1×1 matrix of z components. The 1×1 force constant tensor $K_{zz}^{(ij)}$ for the nth neighbor atoms does not depend on the coordinates, and $\omega(q)$ thus becomes an even function of k which is obtained from

10) Since the longitudinal modes are always in-plane phonon modes, we can omit "i" from iLA or iLO.

the sum of the differential phase factors $e^{i\boldsymbol{q}\cdot\Delta\boldsymbol{R}_{ij}}$.[11] If we consider only the three nearest neighbor atoms, the sum of the differential phase factors is nothing but $f(k)$ obtained in Eq. (2.28) when discussing the electronic structure. The energy dispersion relation thus obtained (see Eq. (2.31)) is an even function of q around the Γ point. The optical out-of-plane transverse branch ($\sim 865\ \mathrm{cm}^{-1}$ at the Γ point in Figure 3.8a) shows a q^2 dependence for the same reason. Thus, there is neither a phase velocity nor a group velocity for the z component of the vibrations at the Γ point, and the phonon density of states shows a step function which is known as a two-dimensional van Hove singularity (see Figure 3.8b). Finally, remember that while Figure 3.8 introduces all the basic concepts of the phonon dispersion in graphene, it is not accurate enough for describing the experimental measurements, mainly for the in-plane optical modes near the Γ and K points. This will be discussed further in Section 3.4.2 and discussed in depth in later chapters of this book.

3.3 Phonons in Nanoribbons

The phonon dispersion for nanoribbons consists of many one-dimensional phonon dispersion relations which can be obtained, as a first approximation, by the zone-folding technique that we discussed in Section 2.2.5. Like for electrons in Chapter 2, we will discuss such a zone-folding procedure when applying it to carbon nanotubes in Section 3.4, which represents a structure where such a procedure is fully applicable because of the cyclic boundary condition. Nanoribbons are terminated at their boundaries, and the zone-folding procedure has to be applied with care.

Some special modes are of interest to Raman spectroscopy. The width breathing phonon mode in which the ribbon width vibrates is a Raman-active phonon mode with A symmetry. This mode originates from the LA phonon mode in graphene.

11) In general, the phase factor $e^{i\boldsymbol{q}\cdot\Delta\boldsymbol{R}_{ij}}$ goes into its complex conjugate if we change $\boldsymbol{q}$ to $-\boldsymbol{q}$. Thus when we change $\boldsymbol{q}$ to $-\boldsymbol{q}$, the dynamical matrix for the z components in a two-dimensional system becomes its complex conjugate. It is clear that $|D^*| = |D|$ for the Hermitian matrix $\mathcal{D}$, and thus the eigenvalues are even functions of $\boldsymbol{q}$ around $\boldsymbol{q} = 0$ (the Γ point). Even though $\omega(\boldsymbol{q})$ is an even function of $\boldsymbol{q}$, a term proportional to $|\boldsymbol{q}|$ might appear in $\omega(\boldsymbol{q})$. For example, for a one-dimensional spring constant model with the force constant, K, we get $\omega(q) = 2\sqrt{K/M}|\sin qa| \propto |q|$, for $(q \sim 0)$. The absence of a linear q term in the phonon dispersion relations along the z axis of graphite comes from the three-fold rotational axis, C_3 along the z direction. Because of this symmetry, $\omega(q_x, q_y)$ should have three-fold rotational symmetry around the C_3 axis. However, no linear combination of q_x and q_y, such as $aq_x + bq_y$ (with constant values for a, b), can be invariant under a $2\pi/3$ rotation around the q_z axis. The simplest invariant form is a constant, and the quadratic form of $q_x^2 + q_y^2$ is also invariant. This is why we get a q^2 dependence for $\omega(q)$ for the out-of-plane branch. When the force constant matrix depends on the atom locations, such as for the in-plane modes, this invariant condition applies to the product of the force constant matrix and the phase difference factor, which generally has a linear q term in $\omega(q)$.

Furthermore, according to the edge structure of graphene nanoribbons, we expect edge-localized phonon modes to appear [131]. Some calculations show that we can see such modes at 1450 cm^{-1} and 2060 cm^{-1} for zigzag and armchair edges, respectively. The reason why we get a relatively lower frequency 1450 cm^{-1} compared to the G-band frequency of 1585 cm^{-1} for the zigzag edge structure is that the edge atoms have only two chemical bonds. In the case of the armchair edge, the dangling bonds of A and B edge atoms form another π bond which makes the C–C bond at the armchair edge a triple bond whose optical phonon modes are around 2000 cm^{-1}. Similar Raman spectra are observed in the polyene C_nH_2, ($n = 8, 10, 12$) encapsulated in a SWNT in the frequency region around 2000 cm^{-1}[4]. When the dangling bonds are terminated by hydrogen atoms, a triple bond becomes a double bond, whose frequency may appear at around 1530 cm^{-1}[132]. The downshift in frequency from 1585 cm^{-1} to 1530 cm^{-1} can be understood by considering the weight of the hydrogen atom. Since the H mass is much lighter than the C mass and since the C–H bond is much stiffer compared with the C–C bond, we may consider that the mass of the edge carbon atoms changes from 12 to 13. In fact, when we multiply $\sqrt{12/13}$ by 1585 cm^{-1}, we get 1530 cm^{-1}. Thus by measuring the micro-Raman modes associated with the edge, we can get information about the edge structure of graphene and related functionalized graphene materials.

3.4 Phonons in Single-Wall Carbon Nanotubes

The vibrational structure of carbon nanotubes is obtained by rolling up the graphene nanoribbon into a cylinder. In this section, we review the zone-folding picture for obtaining the first-approximation to the phonon dispersion relations for nanotubes (Section 3.4.1), while the effect of nanotube curvature is discussed in Section 3.4.2.

3.4.1 The Zone-Folding Picture

As a first approximation, the phonon structure of carbon nanotubes can be obtained using a similar procedure to that used for electrons (see Section 2.3), by superimposing the N cutting lines in the $\boldsymbol{K}_1$-extended representation on the six phonon frequency surfaces in the reciprocal space of the graphene layer [31, 110]. The corresponding one-dimensional phonon energy dispersion relation $\omega_{1D}^{m\mu}(q)$ for the nanotubes is given by:

$$\omega_{1D}^{m\mu}(q) = \omega_{2D}^{m}\left(q\frac{\boldsymbol{K}_2}{|\boldsymbol{K}_2|} + \mu\boldsymbol{K}_1\right), \quad \left(\begin{array}{l} m = 1, \ldots, 6, \\ \mu = 0, \ldots, N-1, \end{array} \text{ and } -\frac{\pi}{T} < q \leq \frac{\pi}{T}\right), \tag{3.19}$$

where $\omega_{2D}^{m}(\boldsymbol{q})$ denotes the two-dimensional phonon dispersion relations for a monolayer graphene sheet, q is a one-dimensional wave vector, T is the magnitude of the one-dimensional translation vector $\boldsymbol{T}$, and μ is a cutting line index.

According to the zone-folding scheme, this procedure yields $6N$ phonon modes for each carbon nanotube. The $6(N/2-1)$ pairs of the phonon modes arising from the cutting lines of the indices μ and $-\mu$, where $\mu = 1, \ldots, (N/2-1)$, are expected to be doubly degenerate, similar to the case of the electronic sub-bands, while the phonon modes arising from the cutting lines for the indices $\mu = 0$ and $\mu = N/2$ are nondegenerate. The total number of distinct phonon branches is $3(N+2)$. For our prototype (4,2) nanotube, $N = 28$, so that there are 90 distinct phonon branches.

Spikes appear in the phonon density of states (DOS) of the carbon nanotube, similar to the spikes (VHSs) appearing in the electronic DOS (see Figure 3.9c), except for the presence of a much larger number of spikes in the phonon DOS than in the electronic DOS, due to the larger number of phonon modes relative to the number of electronic bands, and the more complex structure of the dispersion relations for phonons than for electrons in the graphene layer. However, the spikes in the phonon DOS do not play such an important role in the experimental outcomes as the spikes in the electronic DOS because of symmetry selection rules. Among the large number of the phonon modes in carbon nanotubes, only a few are Raman-active or infrared-active [134, 135]. Further details about the selection rules for the phonon modes are discussed in Chapter 6, where the relevant group theory discussion is presented. The phonon dispersion relations of the graphene layer calculated by the force constant model are shown in Figure 3.9b along with the cutting lines for our (4,2) sample nanotube in Figure 3.9a. The corresponding phonon density of states for the (4,2) nanotube are shown in Figure 3.9c.

3.4.2 Beyond the Zone-Folding Picture

The zone-folding scheme neglects the curvature of the nanotube wall. Meanwhile, the nanotube curvature couples the in-plane and out-of-plane phonon modes of the graphene layer to each other, especially affecting the low frequency acoustic phonon modes. Among the three acoustic phonon modes of the graphene layer, only one of the two in-plane modes results in the acoustic phonon mode of the nanotube corresponding to the vibrational motion along the nanotube axis. The two other in-plane and out-of-plane acoustic phonon modes give rise to the twisting mode (TW, the vibrational motion in the circumferential direction of the nanotube) and to the radial breathing mode (RBM, the vibrational motion in the radial direction of the nanotube), correspondingly, while the two related acoustic phonon modes of the nanotube (the vibrational motion in two orthogonal directions perpendicular to the nanotube axis) can be constructed as linear combinations of the acoustic modes with wave vectors $q = 2/d_t$ [31].

The zone-folding scheme predicts zero frequencies for both the TW and RBM phonon modes of the nanotube at the center of the Brillouin zone ($q = 0, \omega = 0$),

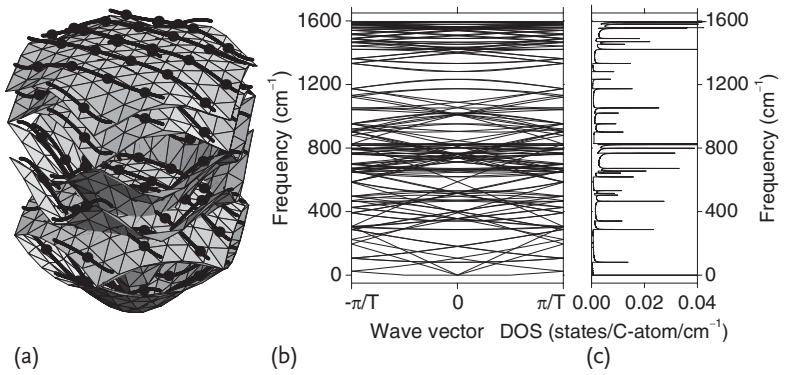

Figure 3.9 (a) The phonon dispersion relations of the graphene layer in the first Brillouin zone calculated with the force constants fitted to the Raman scattering data for various graphitic materials [133]. Solid curves show the cutting lines for the (4,2) nanotube in the fully reduced representation. Solid dots show the ends of the cutting lines in the $\boldsymbol{K}_1$-extended representation. (b) Phonon dispersion relations for the (4,2) nanotube obtained by zone-folding from (a). (c) The density of phonon states for the phonon modes shown in (b) for monolayer graphene [110].

since they arise from the acoustic phonon modes of the graphene layer. However, the RBM phonon frequency cannot have a zero frequency since it is an in-plane, bond stretching phonon mode, though the corresponding TW phonon mode is a bond bending, in-plane phonon mode. In this sense, the RBM mode is not an acoustic phonon mode but an optical phonon mode. The frequency of the RBM is inversely proportional to the nanotube diameter, varying from around 60 to 450 cm^{-1} for typical diameters of 2.0 to 0.5 nm. This was first predicted within the force constant model [123], and then confirmed by resonance Raman scattering measurements [136], and by *ab initio* calculations [137], which also revealed a weak dependence of the RBM frequency on the nanotube chirality. The zone-folding scheme does not explain the characteristics of the RBM [123], although zone-folding does provide better results for the high frequency phonon modes (optical modes), as confirmed by *ab initio* calculations [138]. In order to avoid the limitations of the zone-folding scheme for the low frequency phonon modes, the force constant model can be used directly for the nanotube by constructing and solving the $6N \times 6N$ dynamical matrix for the unit cell of the nanotube, instead of using the 6×6 dynamical matrix for the unit cell of the graphene layer with subsequent zone-folding [31]. Alternatively, the first-principles methods can be used instead of the force constant models to calculate the phonon modes [116, 124], yet the size of the unit cell cannot be too large for *ab initio* methods. Therefore, *ab initio* calculations are presently limited to achiral nanotubes and to only a few chiral nanotubes with relatively small unit cells. Also, the accuracy of the experiments significantly exceeds what *ab initio* calculational methods can presently achieve.

3.5
Beyond the Force Constant Model and Zone-Folding Procedure

The phonon dispersion relations of the graphene layer can be calculated within a force constant model [31], or by tight-binding [139], or *ab initio* [116] methods. In the force constant model, interactions including as many nearest neighbors in the graphene layer can be considered in order to improve the agreement with experiment. The phonon dispersion relations for monolayer graphene can be measured along high symmetry directions in the Brillouin zone by electron energy loss spectroscopy [128], inelastic neutron scattering [123], and inelastic X-ray scattering [129, 130]. The force constants up to the fourth nearest-neighbor were fitted to the phonon frequencies measured by inelastic neutron scattering in graphite [123]. Furthermore, the force constant model using up to 20 nearest neighbor terms were fitted to inelastic X-ray scattering data [140].

Surprisingly, resonance Raman scattering in sp^2 carbons is not restricted to the Γ point ($q = 0$ selection rule), but Raman spectra are also sensitive to the regions around the high symmetry points K (K') in the first Brillouin zone, and this will be discussed in more detail in Chapters 12 and 13. Actually, Raman experiments on sp^2 carbons probing zone center modes provided evidence for a failure of all the force constant, tight-binding and *ab initio* calculational methods used to describe the phonon dispersion relations around these high symmetry points, until the phonon energy renormalization due to electron–phonon coupling was included in the calculations [141].

In the presence of electron–phonon coupling, the phonon lifetime is no longer infinite. When we consider the electron–phonon interaction as a perturbation, the phonon energy can be modified by a virtual excitation of an electron and this effect is significant both for certain Γ and K point phonons. Because of this virtual excitation of an electron, the phonon lifetime becomes finite, and the phonon frequency shows a broadening due to the Heisenberg uncertainty relation. This phenomena generally becomes very strong for the phonon wave vector $q = 2k_F$ where k_F is the Fermi wave vector, and we call this effect the Kohn anomaly effect [141]. In the case of graphene and carbon nanotubes, the Kohn anomaly effect occurs for Γ and K point phonons and we will discuss the effect of the Kohn anomaly on the Raman spectra further in Chapter 8.

Problems

[3-1] Obtain the frequencies of two atoms (of mass M), which are connected to each other by a spring with spring constant K and also connected to the two walls (that is, wall-atom-atom-wall geometry). Here we consider only the longitudinal modes for which the vibration is along the bond axis. We consider that the walls have an infinite mass. Show the two normal modes in a figure, using arrows to show the atomic mode displacements.

[3-2] Obtain the vibrational frequencies of three atoms in similar geometries to the previous problem, which involves the wall-atom-atom-atom-wall geometry. Show the three normal modes using arrows in the figure to denote atom displacements. In order to solve this problem, you can use the fact that any normal mode should be either symmetric or antisymmetric under the inversion operation $x \to -x$.

[3-3] Next we consider $N-1$ atoms attached between the two walls. When we consider x_0 and x_n as the coordinates of the two walls, show that all the equations of motion are expressed by the same formula. Then considering that the Bloch theorem applies, substitute $x_\ell = A\exp(iq\ell a - i\omega t)$ into the equations of motion and obtain the dispersion of the phonon frequency $\omega(q)$. Plot the dispersion of the phonon within the first Brillouin zone.

[3-4] In the previous Problem 3-3, we can use the fixed boundary condition of $x_0 = x_n = 0$. Obtain the $N-1$ q-independent phonon frequency values from the boundary condition.

[3-5] What happens in the previous Problem 3-3, if we adopt the periodic boundary condition $x_0 = x_n$. Here we consider the center of mass motion to be zero.

[3-6] Show that the previous results satisfy the case of $N-1=2$ and $N-1=3$ by comparing your results with answers to earlier questions in Chapter 3.

[3-7] The problems above describe the phonon dispersion for a one-atom per unit cell 1D crystal. If you replace each even atom by a different atom, the system will become a two-atoms per unit cell 1D crystal, with a doubled-size unit cell. Show that the first Brillouin zone is reduced to half the size of the original one and show that the phonon dispersion will be represented by a zone-folding of the one-atom phonon dispersion.

[3-8] In Figure 3.3, choose any unit cell vibrational mode and show that the motion of the atoms for $q = 0$ ($\lambda \to \infty$) and for $q = 2\pi/a$ ($\lambda = a$) is the same.

[3-9] Consider the phonon dispersion of a two-dimensional square lattice with atoms of mass M and spring constant K. Plot the resulting phonon dispersion curve as a function of q_x and q_y.

[3-10] Consider the phonon dispersion of a two-dimensional honeycomb lattice with atoms of mass M and spring constant K. In this case, we have two atoms per unit cell. Show the first Brillouin zone and plot the phonon dispersion for the high symmetry directions within the first Brillouin zone.

[3-11] Consider a $2(N-1)$ linear chain of atoms in which two different atoms A and B with masses M_A and M_B are connected along a chain (wall-A-B-A-B-. . . -B-wall). Obtain and plot the phonon dispersion for this configuration.

[3-12] In the previous problem, show the normal modes for the Γ point and for the zone boundary for each phonon mode.

[3-13] Consider the $2(N-1)$ linear chain with one type of atom (mass M) with two different spring constants alternating in the sequence wall-(K1)-atom-(K2)-...-(K1)-wall. In this case, we have two phonon branches. Plot the phonon dispersion.

[3-14] When we consider a transverse phonon mode, how should we consider the force constant for a linear chain of similar atoms of mass M. Show that stretching a spring in such a linear chain does not give a deformation which is proportional to y or z when we consider the direction along the chain as x.

[3-15] How many normal modes exist for the CH_4, C_2H_2 and C_{60} molecules which, respectively, have the shapes of a regular tetrahedron, a linear chain, and a truncated icosahedron?

[3-16] Let us consider the H_2O molecule. Solve for the phonon normal modes by considering the spring constant K_1 for the H–O bond stretching force constant and K_2 for the H–O–H bond angle force constant. Obtain these force constants by using the experimental values for the mode frequencies.

[3-17] When we consider the two-dimensional square lattice for atoms of mass M and force constant K between nearest neighbor atoms, write an equation of motion for the transverse phonon mode and give a solution for its mode frequency.

[3-18] Let us consider the phonon modes of the C_{60} molecule. When we consider two spring constants for pentagonal and hexagonal C–C bonds, show how to construct the dynamical matrix and how to calculate the phonon modes.

[3-19] Consider zigzag and armchair graphene nanoribbons which have edges with zigzag and armchair shapes. Obtain discrete q vectors in the nanoribbon width direction by defining the width of the nanoribbon.

[3-20] Consider a ring which consists of N carbon atoms, each connected to its neighboring atoms by spring constant K and consider only the radial breathing phonon mode. Then show that the corresponding phonon frequency is inversely proportional to N.

[3-21] When we consider the hexagonal corners of the two-dimensional Brillouin zone of graphene, that is the K and K' points, show that the phonon eigenvectors have the periodicity of a $\sqrt{3} \times \sqrt{3}$ super-cell. How many atoms exist in this super-cell?

[3-22] Consider the previous Problem 3-21 for the case of the M point, which is the center of the hexagonal edge of the two-dimensional Brillouin zone.

[3-23] Study the general theory of the LO and TO phonon modes whose mode frequency ratio depends on the dielectric constant of the materials. In par-

ticular, show that the LO and in-plane TO phonons are degenerate at the Γ point ($q = 0$) in 3D graphite.

[3-24] The sound velocity of the LA phonon mode of graphite is about 21 km/s. Estimate the spring constant of the C–C chemical bond of graphite.

[3-25] Review the principles of inelastic neutron scattering and inelastic X-ray scattering. What is the merit of each of these experimental techniques for studying carbon systems such as graphene and carbon nanotubes?

[3-26] In order to get momentum and energy information from inelastic neutron scattering measurements, we need a monochromator to disperse the neutron beams. How do we get a neutron beam with a fixed kinetic energy?

[3-27] When we use 10 KeV X-rays for observing 0.1 eV phonons, we need high accuracy for observing the scattering angles. Estimate the accuracy of the angles needed for the X-ray detector in such an experiment.